DOI: 10.13009/EUCASS2022-4755
9TH EUROPEAN CONFERENCE FOR AERONAUTICS AND SPACE SCIENCES (EUCASS)

Multi-region thermal characterization in LRE combustion chambers

A. Remiddi[⋆‡], *G. Indelicato*[⋆], *P. E. Lapenna*[⋆†] *and F. Creta*[⋆]
[⋆]*La Sapienza University of Rome*
via Eudossiana 18 - 00184 Rome, Italy
[‡]arianna.remiddi@uniroma1.it · [†]pasquale.lapenna@uniroma1.it
[†]Corresponding author

Abstract

This contribution tackles the thermal characterization problem of a Liquid Rocket Engine combustion chamber under high-pressure operating conditions. The development of an efficient multi-region, multi-physics numerical framework for turbulent combustion and heat transfer modeling is discussed, together with its application on single and multi-injector test cases. The solver features a flamelet-based approach for non-adiabatic, non-equilibrium, non-premixed turbulent combustion, and a consistent Conjugate Heat Transfer description to guarantee the thermal balance across the interfaces between neighbouring continua. The coupling procedure is in particular optimized for convection-dominated phenomena, allowing for the simulation of long time-windows at reasonably limited computational costs.

1. Introduction

Thermal characterization is one of the fundamental aspect in the design process of a propulsion system, directly affecting both the operating life and performance, and also preventing the occurrence of thermo-mechanical failures. This problem becomes of particular relevance when dealing with Liquid Rocket Engines (LREs), a widespread technology in the space industry that is undergoing a deep innovation process to meet, besides the usual requirements of high performance, limited budgets and reduced developing time, also the recently rose requirement of reusability, since LREs are sought as major candidates for Reusable Launch Vehicles (RLVs). Combustion modelling is a complex and interrelated topic in itself, involving the interplay of a plethora of multi-physics and multi-scale phenomena, ranging from the turbulent mixing of the reactants to the convective and radiative heat transfer. Moreover, in the context of LREs the issue of thermal characterization is even less lacking in challenges: not only the high-pressure conditions under which combustion typically occurs escalates the thermal load on the combustion chamber walls, but also causes the propellants to approach the so-called trans-critical state, a condition characterized by highly non-linear behaviour and real-gas effects which therefore requires proper understanding and modelling.[15] If to this is added the description of the interaction between different engine components, such as the cooling system, it becomes clear the intrinsically stiff and multi-physics nature of the thermal characterization problem. Such a problem can be efficiently tackled by Computational Fluid Dynamics (CFD), that is increasingly replacing experiment in the early design stages, also thanks to the growing capability of the High Performance Computing (HPC). In this contribution a newly developed numerical framework for the description of turbulent, non-premixed combustion and heat transfer across different continua is presented, aiming at the characterization of a combustion chamber complete with its cooling system in LRE-like conditions. The multi-region solver tackles simultaneously multiple solid and fluid domains, coupling them at the interface with a condition representative of the heat exchanged. It relies on several modeling strategies to handle the multi-scale problem and reduce the stiffness induced by the finite rate kinetics of turbulent combustion and that induced by acoustics and boundary layers in the combustion chamber. Further details on the employed models will be given in the following section.

Concerning the coupling between neighbouring continua, two main approaches are usually found in the literature. The first category goes under the name of *direct coupling* and enforces the Conjugate Heat Transfer (CHT) condition, prescribing the continuity of heat flux and temperature across the interface at each iteration. Although the high fidelity of the description, this approach is penalized by the high computational cost needed to handle the coupling of all the involved time scales, and to the best of the authors knowledge, it is used in LRE-like conditions only for simple configurations of mono-species coolant flows.[18] The second class of models is referred to as *loose coupling* and is characterized by the enforcement of a thermally chained description, i.e. the simulation of a single domain at time

DOI: 10.13009/EUCASS2022-4755

followed by the enforcement of the results as a boundary condition to the other domain. The procedure is based on a first-guess solution and is iterated until convergence.[13,16] Some examples are present in the literature of the two approaches used simultaneously in actively cooled combustion chambers: for those configurations the direct coupling is enforced between the coolant flow and the solid wall, while a thermal chaining technique is employed to couple the solid structure with the hot gas side. In particular Song et. al[23] and Rahn et al[19] resort to the iterative imposition of temperature, while Betti et al[1] enforce a condition on the heat transfer coefficient.
The multi-region, multi-physics solver presented in this contribution envisages a CHT description for both the high-pressure turbulent combustion and heat conduction through the solid walls, moving therefore a step further compared to the aforementioned works. In order to minimize the computational costs for extremely stiff problems, an alternative coupling strategy is also formulated stemming from the loosely coupled methods. An experimental combustion chamber[2] is chosen as test bench both in two- and three-dimensional settings. The simulation of a three-dimensional multi-injector combustor[16] is also presented, in order to show the framework capability on more complex configurations.

2. Numerical framework

The numerical framework for turbulent combustion and heat transfer modeling presented in this contribution is based on the open-source frameworks OpenFOAM[8] and OpenSMOKE++.[3] It can tackle simultaneously an arbitrary number of solid and fluid domains, solving the respective governing equations in a segregated strategy and coupling them at the interface through a condition guaranteeing the continuity of temperature and heat flux. In the following subsections the governing equations and the modeling strategies exploited are presented.

2.1 Governing equations in the solid domains

The thermal conduction within solid walls is modeled in the solver resorting to the Fourier equation:

$$\frac{\partial(\rho h)}{\partial t} = \frac{\partial}{\partial x_j}\left(\alpha \frac{\partial h}{\partial x_j}\right) \tag{1}$$

Where h is the enthalpy, ρ is the density and α is the thermal diffusivity. The description of porous and anisotropic continua is easily implemented in the solver through the introduction of proper correction factors to the diffusivity α. It is also possible to account for variable conductivity across the solid width.

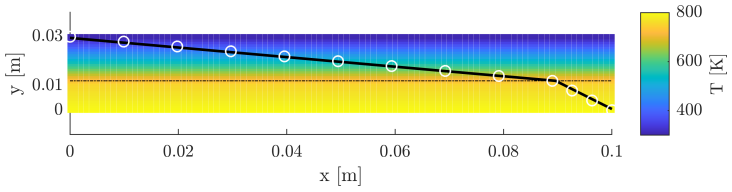

Figure 1: Multi-layer wall. The color code and the solid line represent the temperature field resulting from the coupled simulation, compared to the analytical solution (white markers).

A simple multi-layer wall with different temperatures at the boundaries has been used as validation test case for the governing equations in the solid domains, as reported in Fig. 1. The temperature field on a section of the mentioned multi-layer wall after the attainment of the steady state condition has been compared to the well-known analytical solution, showing perfect agreement.

2.2 Governing equations in the fluid domains

The non-premixed, turbulent combustion modeling problem is handled in the fluid domains with a tabulated chemistry approach coupled with a RANS fluid-dynamic solver.
The former is used to decouple the thermo-chemistry problem from the fluid-dynamic mixing and allows for a reduction of the overall computational costs. The idea is to represent the thermophysical properties of the fluid as function of a conserved scalar Z, store those in libraries in a pre-processing step[17] and finally solve a transport equation for the conserved scalar in addition to the traditional Navier-Stokes equations. The approach is amenable for the description of both multi-species reacting mixtures and mono-species flows, making it possible to model simultaneously both

DOI: 10.13009/EUCASS2022-4755

reaction on the hot gas side and non-reacting flows in the cooling system. In the case of chemically reactive flow the conserved scalar Z is called mixture fraction and is representative of the local composition, while for mono-species flows it is defined as a non-dimensional temperature. The libraries containing the thermophysical quantities mapped on the conserved scalar Z are also known as *flamelet*, and are parametrized also by the stoichiometric scalar dissipation χ_{st}, representative of the distance from the equilibrium, and by the enthalpy defect ϕ_H, used to account for non-adiabatic effects.[9, 10, 14]

In order to have a preliminary validation of the fluid-dynamic solver, a mono-species, laminar benchmark backward facing step from the literature[20] has been successfully reproduced, as shown in Fig. 2, where the coupled solution obtained has been compared to both the literature results and the solution obtained with a native OpenFOAM solver for Conjugate Heat Transfer.

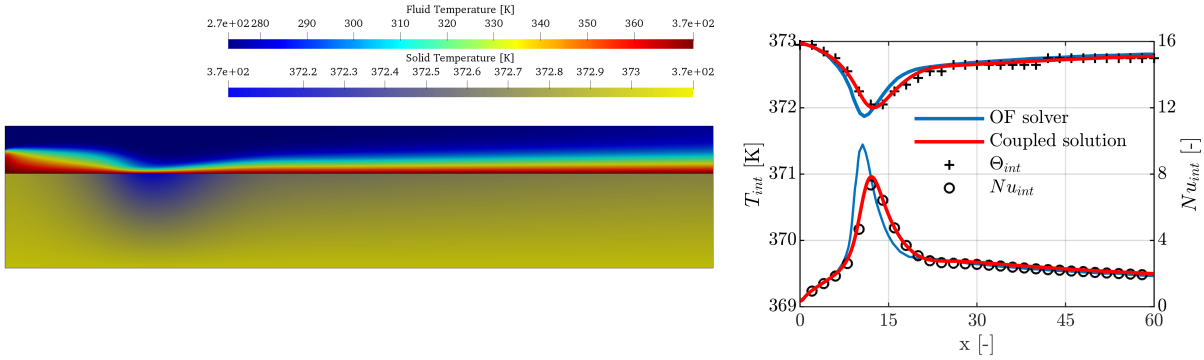

Figure 2: Mono-species laminar backward facing step. Left panel: configuration coloured with the temperature field. Right panel: non-dimentional temperature and Nusselt number at the interface, comparison between the coupled solution, the literature data and the solution obtained with the native OpenFOAM solver for CHT.

The solver is amenable for the modeling of both laminar and turbulent flows, allowing for the simulation of a wide range of possible configurations. Turbulence effects are introduced through the use of presumed-pdfs, in particular β-pdf for Z, and Delta-dirac distribution for both χ and ϕ_H.[9, 11, 12] For the test cases considered in the following, the $k-\epsilon$ model is used with standard coefficients.

In the most general case, i.e. turbulent and chemically reactive, the generic Favre-averaged thermochemical variable $\widetilde{\psi}$ is expressed as:

$$\widetilde{\psi} = \widetilde{\psi}(\widetilde{Z}, \widetilde{Z''^2}, \widetilde{\chi_{st}}, \widetilde{\phi}) \tag{2}$$

In particular, the turbulent, multi-species flamelets used in this work are based on the so-called frozen assumption, according to which enthalpy losses only affect the temperature field within the boundary layer, while the composition is kept fixed and equal to the adiabatic one.[6]

The transport equations for the Favre-averaged mixture fraction $\widetilde{Z}$ and its variance $\widetilde{Z''}$ in the multi-species and turbulent setting are expressed as follows:

$$\frac{\partial(\rho\widetilde{Z})}{\partial t} + \frac{\partial(\rho\tilde{u}_i\widetilde{Z})}{\partial x_i} = \frac{\partial}{\partial x_i}\left[\left(\alpha + \frac{\rho\nu_t}{Sc_t}\right)\frac{\partial\widetilde{Z}}{\partial x_i}\right] \tag{3}$$

$$\frac{\partial(\rho\widetilde{Z''^2})}{\partial t} + \frac{\partial(\rho\tilde{u}_i\widetilde{Z''^2})}{\partial x_i} = \frac{\partial}{\partial x_i}\left[\left(\alpha + \frac{\rho\nu_t}{Sc_t}\right)\frac{\partial\widetilde{Z''^2}}{\partial x_i}\right] + C_g\left(\alpha + \frac{\rho\nu_t}{Sc_t}\right)\left|\frac{\partial\widetilde{Z}}{\partial x_i}\right|^2 - C_d\rho\frac{\epsilon}{k}\widetilde{Z''^2} \tag{4}$$

Some other modeling strategies are exploited to reduce the stiffness of the problem: the unsteady RANS (uRANS) equations are solved in a low-Mach number approximation, and a modified version of the wall function developed by Han and Reitz[4] which has been recently validated in the context of LRE[6] is used to bridge the near-wall field with the fully turbulent flow and avoid the costly solution of the boundary layer reducing the grid requirement at the walls.

The framework presented in this section is based on a pre-existing version of a single-region fluid-dynamic solver, largely validated in a variety of applications featuring LRE-relevant conditions.[5, 7, 21, 22]

DOI: 10.13009/EUCASS2022-4755

2.3 Domains coupling

The proposed multi-region solver activates specific section of the code depending on whether the domain being solved is fluid or solid. Such domains are then coupled at the interface by means of a thermal boundary condition prescribing heat flux and temperature continuity.
In the case of direct coupling, the CHT condition is operatively expressed as the balance equation reported in Eq. 5:

$$\begin{cases} T_{F,int} = T_{S,int} = T_{int} \\ \lambda_F \frac{T_F - T_{int}}{\Delta y_F} = \lambda_S \frac{T_{int} - T_S}{\Delta y_S} \end{cases} \tag{5}$$

where the subscripts F, S and int respectively stand for fluid, solid and interface, λ is the thermal conductivity of the considered continua and Δy is the distance between the interface and the first cell centre in the domain, as briefly depicted in Fig. 3.

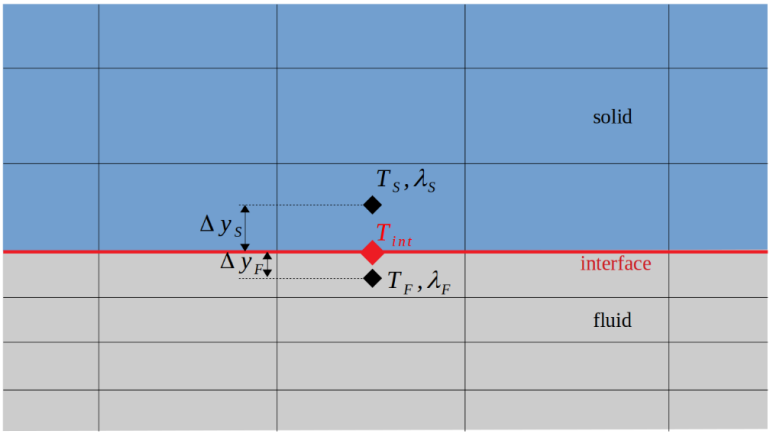

Figure 3: Schematic view of the interface between solid (blue) and fluid domain (gray).

The enforcement of the condition reported in Eq. 5 results in a constraint for the unknown interface temperature:

$$T_{int} = T_{nbr}\left(\frac{\lambda_{nbr}\Delta_{nbr}}{\lambda_{my}\Delta_{my} + \lambda_{nbr}\Delta_{nbr}}\right) + T_{my}\left(1 - \frac{\lambda_{nbr}\Delta_{nbr}}{\lambda_{my}\Delta_{my} + \lambda_{nbr}\Delta_{nbr}}\right) \tag{6}$$

Equation 6 is calculated at each numerical iteration, guaranteeing the direct coupling between the domains. Here, following the OpenFOAM notation, subscripts *my* and *nbr* (neighbour) indicate respectively the interface side from which T_{int} is calculated and the adiacent one, and Δ is the inverse of Δy.
The tabulated chemistry approach used allows to maintain unvaried Eq. 6 for all the possible flows conditions, i.e. turbulent and/or laminar and mono- and/or multi-species. The fluid conductivity λ_F is in fact directly read from the tables, retaining by definition the information about the local composition and the eventual effective value $\lambda_{F_{Eff}}$, which namely is the summation of the laminar and turbulent terms.
The major drawback of the CHT condition presented above is the significant computational cost due to the strong coupling between all the involved time scales, that makes the solution of the entire problem to be driven by the most demanding issue, i.e. the time-integration of the fluid-dynamic field. The severity of the problem becomes of particular concern when the latter includes some complex features as in the case of turbulent mixing and combustion, and even more for applications which do not present a thermal steady-state, and for which is therefore not even possible to initialize the numerical simulation in a near-equilibrium configuration to speed up the convergence. In this respect, a configuration which can be considered particularly demanding is a capacitively cooled combustor, for which the heat transfer problem is intrinsically transient.
A different coupling strategy can be exploited to mitigate the computational cost of these configuration, based on the strengths of both the direct and loose coupling approaches, and on the property of the capacitively cooled cases of being convection dominated. Taking advantage of the overriding effect of the fluid-to-solid heating with respect to the solid-to-fluid cooling, this strategy aims at interrupting the simulation of the chemically reactive flow neglecting the cooling effect exert by the solid wall, and at representing the hot gas side heating effect by means of a proper boundary condition. The idea is to start the simulation with the CHT boundary condition (Eq. 5), inheriting from the *direct*

DOI: 10.13009/EUCASS2022-4755

coupling approaches the absence of initial assumption and the high fidelity of the description. When the flow field reaches a statistical steady state, the interface condition can be replaced by the Newton condition expressed as in Eq. 7:

$$h_C\,(T_{ad} - T_{int}) = \lambda_S \frac{\partial T_S}{\partial y}\bigg|_{\text{int},y=-0} \tag{7}$$

$$h_C = \frac{q}{T_{ad} - T_w} \tag{8}$$

where h_C is the convective heat transfer coefficient defined as in Eq. 8 and calculated on the basis of the directly coupled simulation, while T_{ad} is the interface temperature of the corresponding adiabatic simulation. Both the quantities can be considered as time-independent reference parameters: the former is shown to attain a steady-state value after an initial transient (cfr. next section), and the latter is only depending on the fixed injection conditions. The enforcement of the Newton condition is inherited from the *loose coupling* approaches and allows to proceed on the solid conduction time scale, resulting in a significant reduction of the computational costs and times. In particular, the use of a h_C condition, rather than a temperature or heat flux one, has also been suggested by Betti et al,[1] due to its weak dependence on the unknown T_{int}. A schematic overview of the coupling strategy is given in Fig. 4.

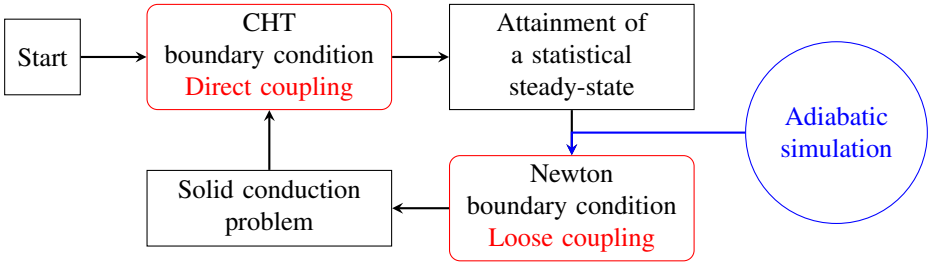

Figure 4: Flowchart of the coupling strategy

3. Results

The employment of the previously introduced coupling strategy allows for the simulation of complex configurations in time frames of industrial and laboratory interest. In this section two experimental capacitively cooled combustors[2,16] developed at the TUM - Technical University of Munich are taken as reference test cases.

3.1 Single injector test case

The TUMrig combustor[2] is an experimental combustion chamber used as reference test case by a plethora of groups in the rocket community[6,13,16,21,22,25] and consisting in a square-section chamber equipped with a single shear coaxial injector and capacitively cooled by means of oxygen-free copper walls (Cu-HCP, high conductivity phosphorous copper). The injector is emanating a non-premixed gaseous oxygen - gaseous methane flame.

3.1.1 Two-dimensional setting

For this case a load point of $p = 20bar$ and an $OF = 2.6$ is taken as a reference, based on the work by Celano et al.[2] Given the axial symmetry of the configuration, an initial two-dimensional approximation is used in a first instance. In order to do this, appropriate equivalent radii have to be defined to represent the equivalent cylindrical chamber: the equivalent radius for the fluid domain is defined in order to maintain the mass-flow rate, while for the solid domain an equivalent annulus has been defined in order to maintain the total mass. While the solid domains length comprises the injection ducts, the combustion chamber and the nozzle as well, the fluid domain is truncated in correspondence of the nozzle inlet. This choice allows to avoid the heat confining in the ending portion of the solid wall, while being consistent with to the low-Mach hypothesis under which the work is carried. A schematic view of the configuration is shown in Fig. 5, together with a representation of the boundary condition imposed: the interface condition is applied on both the chamber lateral wall and injection plate, while a natural convection condition is enforced on the solid external wall, making reference to an external ambient temperature of $T_{air} = 290K$ and a convective heat transfer coefficient $h_{C_{air}} = 10W/m^2K$. All the other walls are considered adiabatic, following the work of Perakis and Haidn.[16]

DOI: 10.13009/EUCASS2022-4755

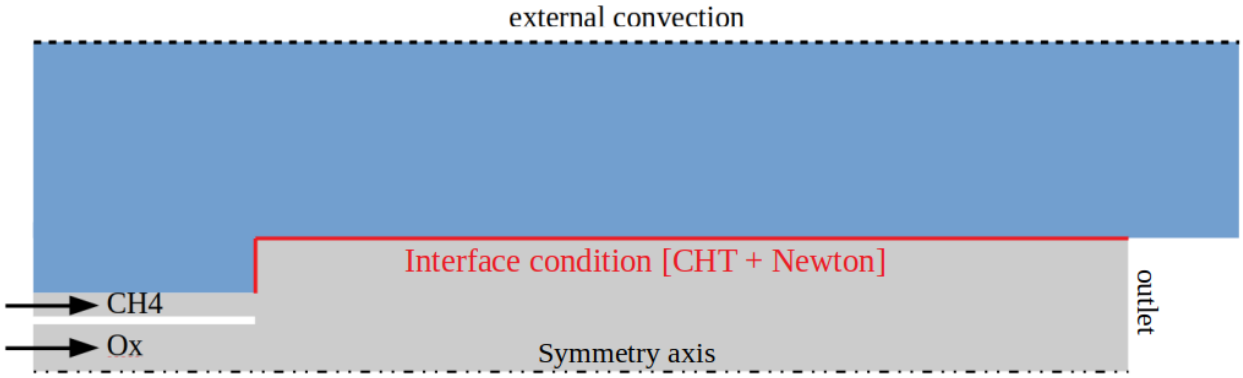

Figure 5: Boundary conditions settings.

On the interface patches the coupling strategy based on the alternation between CHT and Newton condition has been deployed, allowing for the simulation of the entire duration of the experimental run. Figure 6 shows the temperature field in the coupled domains after 3 seconds of burning time, corresponding to the experimental shot.

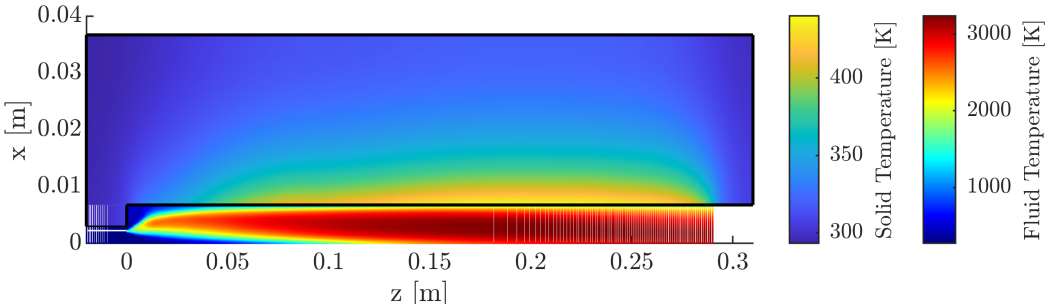

Figure 6: TUMrig combustion chamber configuration. Axes not to scale.

An extensive grid convergence analysis has been conducted, analyzing the results obtained on four different numerical grids obtained on from each other doubling the number of computational points in each direction. Figures 7 and 8 show respectively those results on the combustor lateral wall and injection plate, with the corresponding grids labelled in order of increasing refinement level. In both cases, the left panel shows the temperature profile obtained at a fixed time instant on the entire wall, while the right panel shows the temperature evolution in units of flow-through times for a fixed abscissa. It is possible to observe the attainment of an asymptotic convergence, based on which the TUM3 grid has been chosen as baseline grid, representing a trade-off solution between accuracy and cost-effectiveness.
Results shown up to now are obtained with the fully-coupled CHT interface condition. Once defined the baseline numerical grid with the most accurate set of boundary condition possible, we will now focus on a time convergence analysis to validate the usage of the Newton condition. Figure 9 shows the heat transfer coefficients on both the combustor lateral wall and injection plate, obtained by performing the simulation with the prescribed boundary condition for approximately 20 flow-through times. In particular, the left panels show the coefficient calculated on the patches for several time instants, while on the right time-averaged h_C values are reported in units of flow-through times for specific abscissas. It can be observed that the coefficients progressively collapse onto a steady-state condition already after 5 flow-through times, and that the approximation of constant h_C used in Eq. 7 is therefore acceptable.
The directly coupled simulation has been continued beyond 18 flow-through in order to provide a reference for the interface temperature calculated with the Newton condition. Figure 10 reports the results obtained according to the two methods on overlapping time instants, showing that the Newton condition provides a good approximation of the CHT interface.
The implementation of the aforementioned coupling strategy has allowed for the simulation of the entire experimental run, consisting in 3 seconds of burning time followed by 6 seconds of chamber quenching, the latter being modeled

DOI: 10.13009/EUCASS2022-4755

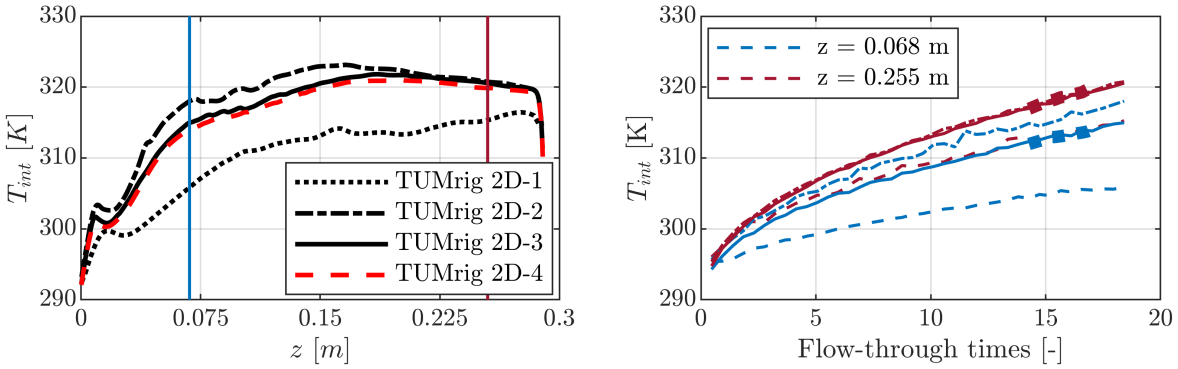

Figure 7: Grid convergence: chamber wall interface temperature at given time (left panel) and temperature evolution in time for several grids sampled at two fixed control stations.

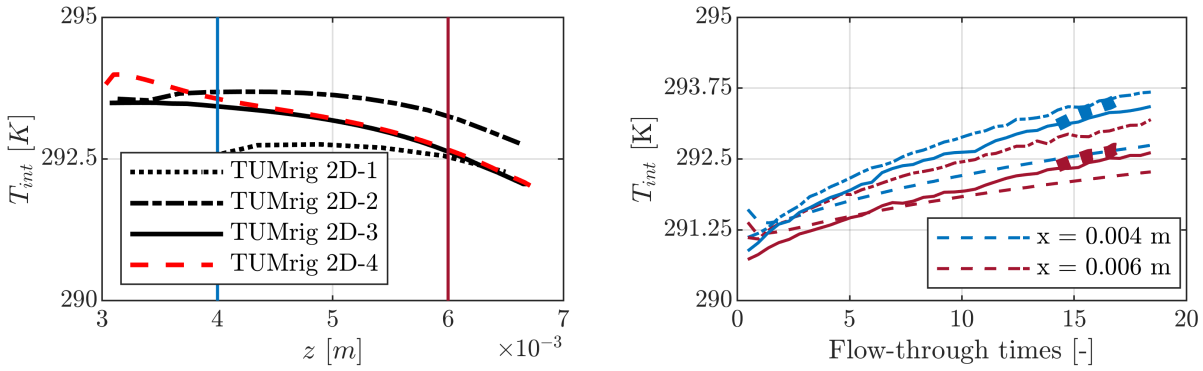

Figure 8: Grid convergence: injection plate interface temperature at given time (left panel) and temperature evolution in time for several grids sampled at two fixed control stations.

through the prescription of a zero heat flux condition at the interface. Comparison with experimental and literature results will be carried out in the following, limitedly to the combustor chamber lateral wall, due to the absence of experimental measurements and literature data on the injection plate. Figure 11 shows in the left panel the heat flux calculated at the end of the burning time, compared to experimental results[2] and literature data.[6,16] Results from Indelicato et al[6] refers to two- and three-dimensional simulations performed with the single-region version of the fluid-dynamic solver used in this work, under equal injection conditions and bounded with an isothermal boundary condition. The comparison with those results highlights the effect of having introduced a coupled description: although having used experimental data for the isothermal simulations, it is possible to see that the predicted heat flux is higher with respect to the coupled case, due to the fact that the transient heating of the solid wall is neglected by the isothermal assumption.

The right panel of Fig. 11 shows the temporal evolution of temperature in correspondence of the experimental thermocouples. Following what described in the experimental work by Celanno et al,[2] temperature data has been sampled at a distance of 1 mm from the fluid-solid interface, accounting therefore also for the damping effect of the solid conduction. An overall good agreement is observed. An underestimation of the results is observed in the chamber shutoff phase, due to the harsh modeling assumption employed. Imposing a zero heat flux condition, in fact, neglects the residual heat exchanged with the hot burnt gases after the shut off of the combustion chamber, and results in a faster cooling down as it is demonstrated by the steeper temperature slope.

3.1.2 Three-dimensional setting

The TUMrig combustor has been investigated also in a three-dimensional setting, making reference for this case to a load point $p = 20bar$ and an $OF = 3.0$, in order to match the work by Perakis et al.[16,24] The boundary condition settings are retained from the two-dimensional simulation, as previously shown in Fig. 5. The employed numerical grid consists in 10^6 finite volumes for the fluid domain and $6 \cdot 10^6$ for the solid region and derives from the previous single-region grid largely validated in.[6]

DOI: 10.13009/EUCASS2022-4755

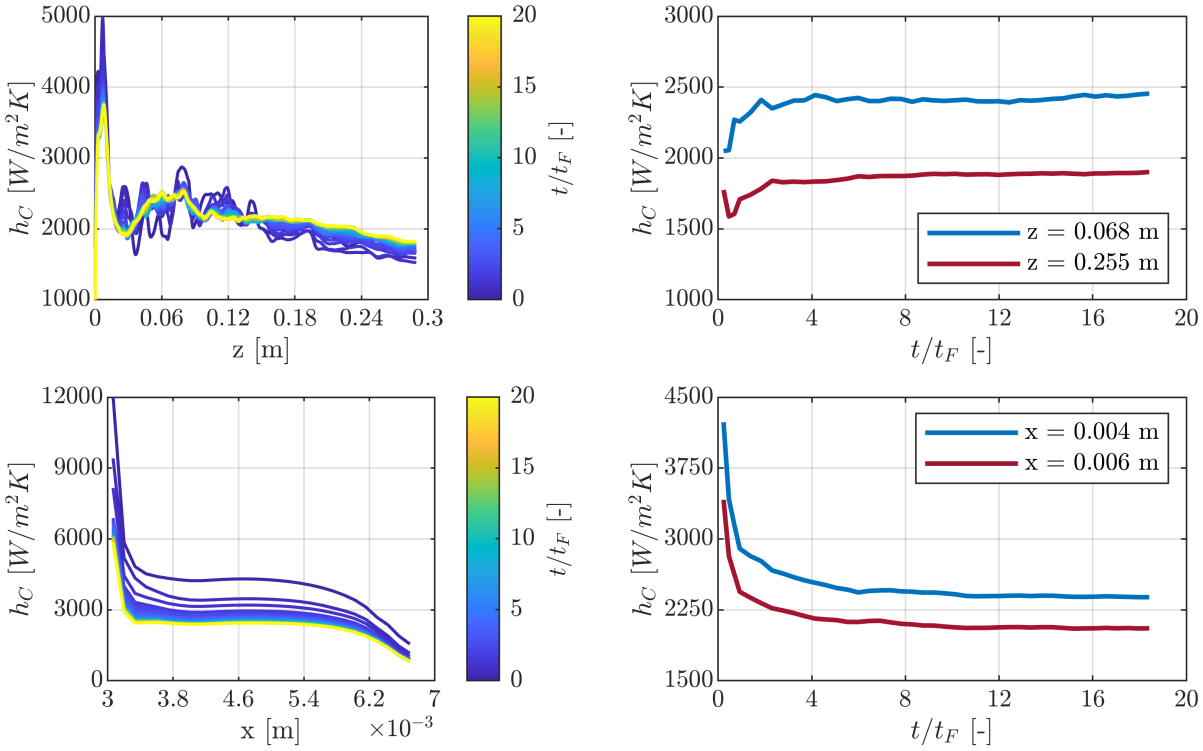

Figure 9: Convergence of the heat transfer coefficient to a steady value on the combustion chamber lateral wall (top) and injection plate wall (bottom). On the left h_C is shown for the entire wall, while right panels show the coefficient evolution in units of flow-through time for several abscissas taken as control stations.

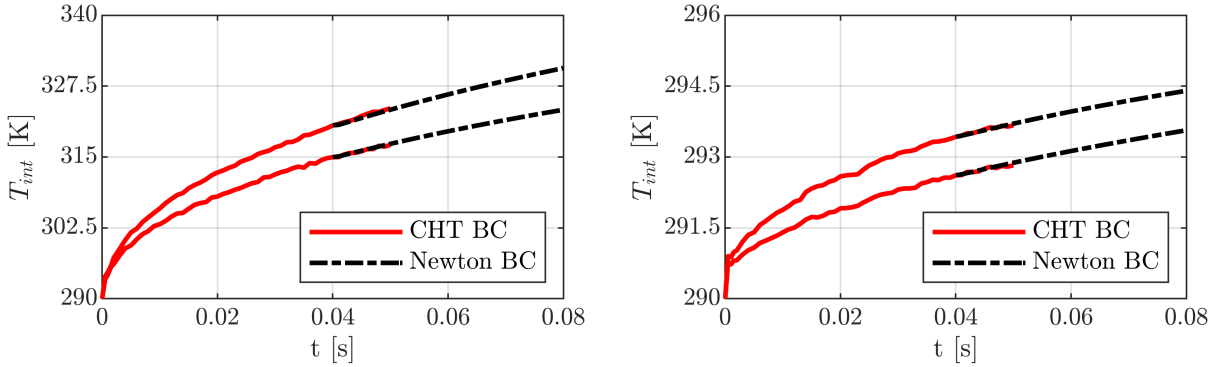

Figure 10: Continuity of the interface condition in terms of interface temperature evolution in time at several abscissas, for the lateral wall (left) and injection plate (right).

As for the two-dimensional case, it has been first verified that h_C attains a steady-state value. Based on what learnt with the previous case, it has been possible to simulate a shorter time interval: a satisfactory constant value is observed to be already attained after two flow-through, as reported in the left panel of Fig. 13. Also in this case, the directly coupled simulation has been performed for some other time instants in order to provide a reference for the interface temperature calculated with the Newton condition. Results are shown in the right panel of Fig. 13, confirming again the validity of the coupling strategy.

The entire duration of the experimental run has been therefore simulated applying the Newton interface condition, results are compared in the following to the reference data published by Perakis and Haidn in.[16] The temporal evolution of temperature for several thermocouples locations is reported in Fig.14. An overestimation of the temperature for the abscissas located in the central region of the chamber is found, as already observed in Fig. 11 and in the work by Indelicato et al.,[6] where this effect has been ascribed to the wall modeling employed. On the other hand, data sampled in the initial and ending sections of the combustion chamber are in satisfactory agreement with the literature data. The

DOI: 10.13009/EUCASS2022-4755

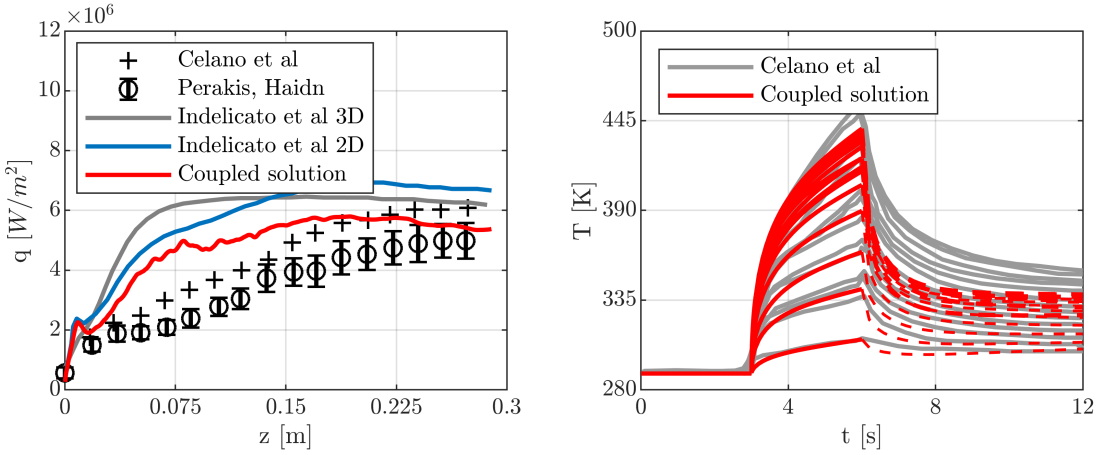

Figure 11: Left: Heat flux at the interface compared to experimental and literature data at the end of the experimental run. Right: Temperature evolution in time compared to the thermocouples readings

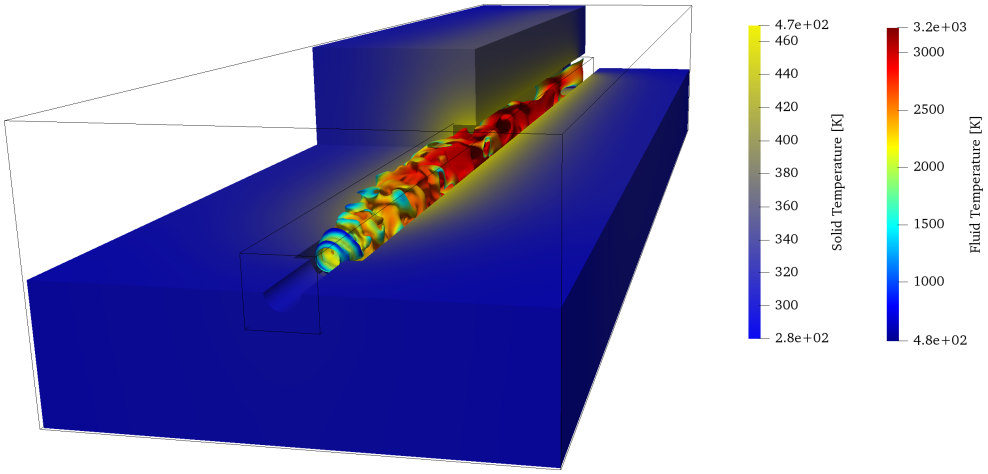

Figure 12: 3D single injector with instantaneous isosurface of stoichiometric mixture fraction colored by temperature.

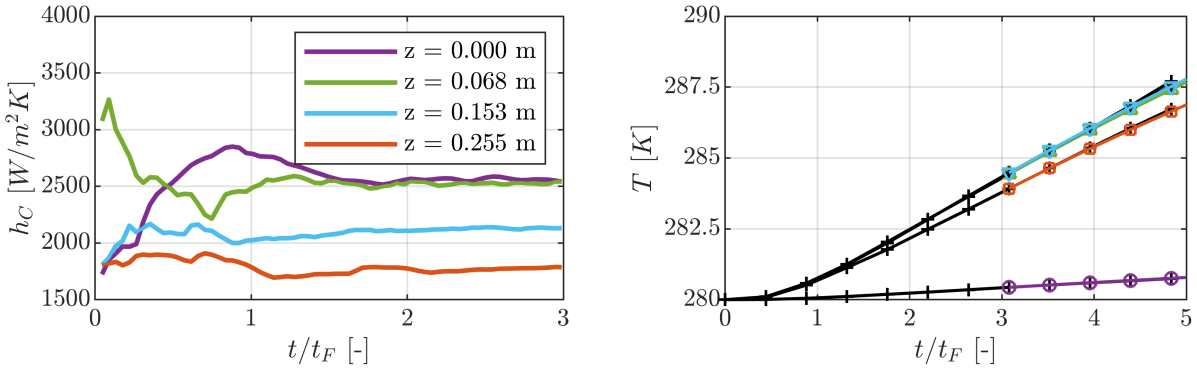

Figure 13: Assessment of the interface coupling strategy. Left panel: Attainment of a steady state value of h_C in the 3D single-injector configuration. Right panel: Equivalence of temperature calculated using CHT (black) and Eq. Newton compared at several thermocouples locations (color coded).

measuring point nearest to the outlet section is affected by a slight underestimation of the final temperature value, this phenomenon was already observed by Maestro et al[13] and is ascribable to the enforcement of the adiabatic condition

DOI: 10.13009/EUCASS2022-4755

over the solid surfaces corresponding to the nozzle. The evaluation time window highlighted in Fig. 14 is used to obtain time-averaged field within the solid domain, following what done in.[16] A slice of such domain is presented in Fig. 15, showing a satisfactory agreement with the reference data.

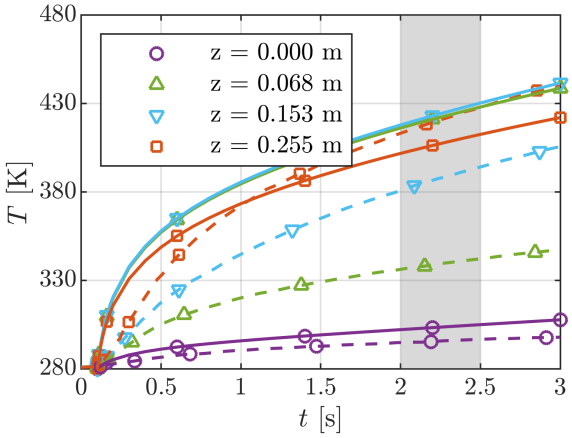

Figure 14: Temperature evolution in time for several thermocouples. Results of the coupled simulation (solid lines) compared to results form[16] (dashed). The vertical band highlights the evaluation time.

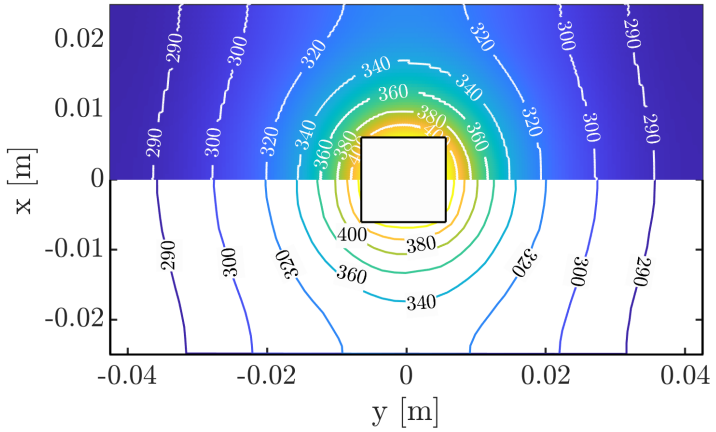

Figure 15: Temperature field in the solid domain at z = 0.255 m averaged over the evaluation time. Comparison between results from the coupled simulation (top) and by Perakis and Haidn[16] (bottom).

3.2 Multi-injector test case

A three-dimensional multi-element combustor has been finally simulated to provide an example of complex configuration of industrial relevance that can be handled by the proposed solver. The assembly consists in a rectangular combustion chamber developed again at the TUM - Technical University of Munich, equipped with five aligned injectors identical to the previous single-element case, and is capacitively cooled with oxygen-free copper walls as in the previous case. The load point considered refers to a pressure of $p = 20bar$ and an oxidizer-to-fuel ratio of $OF = 3.4$, following the reference work.[16] The grid resolution is the same of the three-dimensional single-injector test case, and also the set up of the boundary condition is retained from the previous section. An overview of the configuration is given in Fig. 16.

Figure 17 shows the convergence of the heat transfer coefficient h_C to the steady-state value. In this case the control stations are taken at several location both along the longitudinal direction (color code in Fig. 17) and along the spanwise direction. The combustion chamber is in fact equipped with several thermocouples named 1C, 2C, 3L, 3C, 3R, 4C, 5C, with C indicating the sampling points above an injector element and L and R respectively the position on

DOI: 10.13009/EUCASS2022-4755

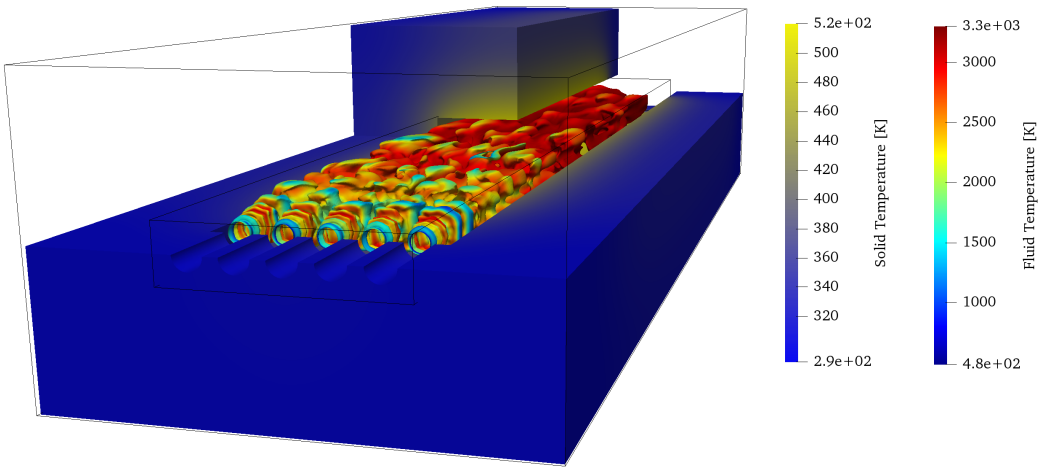

Figure 16: 3D multi injector with instantaneous isosurface of stoichiometric mixture fraction colored by temperature

the left and on the right of the central injector,[16] for the sake of brevity and taking advantage of the symmetry of the configuration, only data taken from the left-side of the configuration are displayed.

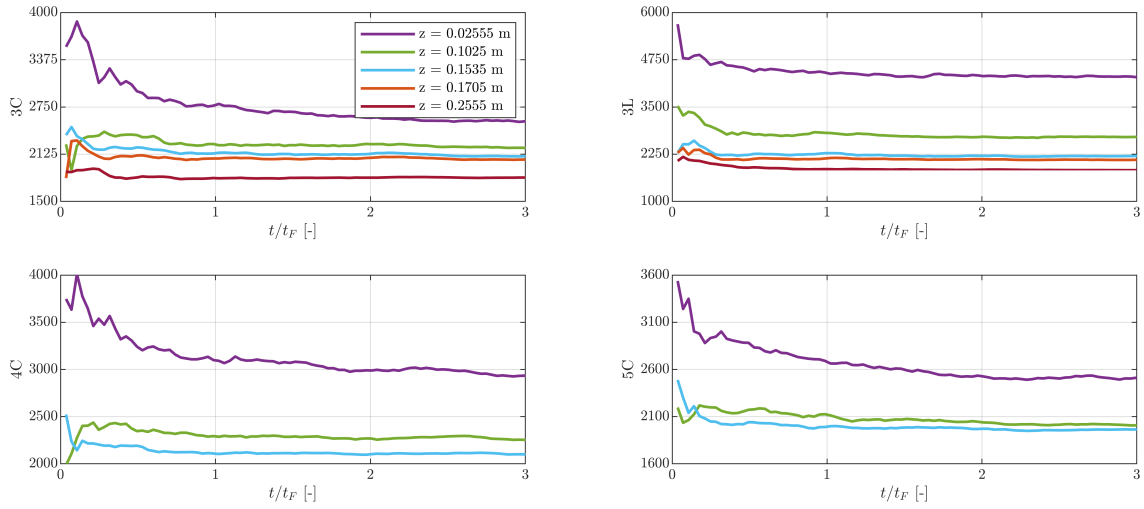

Figure 17: Attainment of a steady state value of h_C in the multi-injector configuration.

Resorting to the enforcement of the Newton boundary condition, the entire duration of the experimental burning time has been simulated. Figure 18 shows the temperature profile for several abscissas at the evaluation time, compared to both the experimental data and the results of the inverse method presented by Perakis and Haidn in.[16] Once again, an overestimation of the results is found for the thermocouples located in the central section of the combustor, as already observed in the previous subsections. Conversely, data sampled in correspondence of the furthest thermocouple location are significantly underestimated, due to the proximity to the outlet section ($z = 277mm$). As previously mentioned, the enforcement of an adiabatic condition in correspondence to the nozzle neglects the high temperatures that the solid would withstand if the expanding flow was simulated, and lead to an underestimation of the temperature field in the ending portion of the chamber. Finally, the temperature field averaged over the evaluation time (between 2 and 2.5 s) in a section of the solid domain sampled at $z = 0.230$ m is shown in Fig. 19. A qualitative comparison with the results obtained in[16] is performed. Note that the reference comparative results are sampled at $z = 0.2725$ m, but it has been decided to not use the same abscissa, in order to avoid the underestimation observed in proximity of the outlet. Due to the difference in the sampling locations, the comparison can be only limited to the temperature field patterns.
The temperature field averaged over the evaluation time (between 2 and 2.5 s) in the solid domain is shown in Fig. (19),

DOI: 10.13009/EUCASS2022-4755

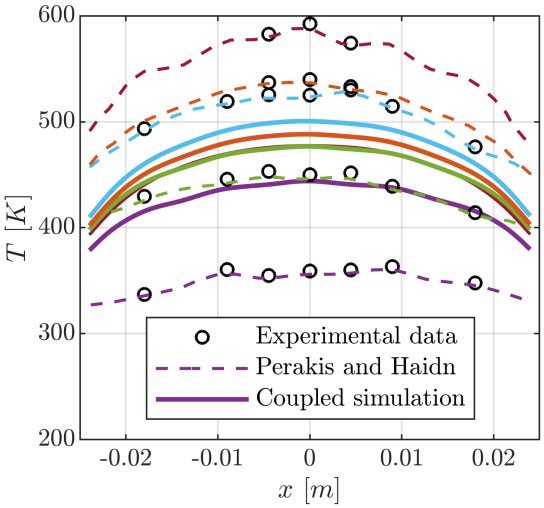

Figure 18: Interface temperature for several abscissa at the evaluation time, compared to Perakis inverse method and experimental data.[16] Color legend from Fig. (17) to represent the thermocouples abscissas.

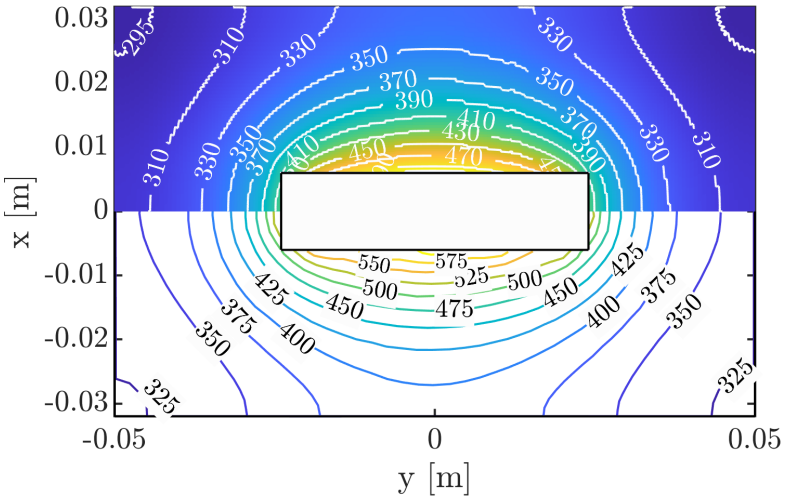

Figure 19: Temperature field in the solid domain at z = 0.230 m averaged over the evaluation time. Comparison between results from the coupled simulation (top) and those obtained by Perakis and Haidn[16] at z = 0.273 m (bottom).

together with a qualitative comparison with the data presented in.? Note that the section sampled at z = 0.2725 m in? has been compared here to a section sampled at z = 0.230 m, chosen as a representative section not affected by the underestimation observed in proximity of the outlet. Any further difference in the presented results can be ascribed to a difference in the solid initial temperature leading to a comparison that should be therefore limited to the temperature field pattern.

4. Conclusions

In this contribution a multi-region and multi-physics solver for time-resolved turbulent combustion and heat transfer modeling is presented, together with its application on a number of different test cases. The solver tackles multiple solid and fluid domains, prescribing temperature and heat flux continuity across the interfaces, and aims therefore at being predictive over the wall thermal characterization. Several modeling solutions are enforced in order to limit the overall computational effort. Among these, a flamelet-based approach is used to solve the thermo-chemical problem of turbulent non-premixed combustion in a pre-processing step, and a wall-modeled description allows to avoid the solution of the thermal boundary layer. The coupling strategy between different continua is based on a consistent

DOI: 10.13009/EUCASS2022-4755

Conjugate Heat Transfer description, optimized in a second instance for convection-dominated problem through the introduction of an alternative coupling strategy. Three experimental run of capacitively cooled combustor have been reproduced with limited computational effort to assess the capability of the solver, showing overall promising results.

5. Acknowledgments

The authors Italian Super Computing Center CINECA for the computational resources accessed trough the ISCRA-C Project HP10CN0S3R. A. R. acknowledges the support of the Italian Ministry of University and Research (MUR). G. I. acknowledges the support of Lazio region in the context of "POR FESR LAZIO 2014-2020". The support of Sapienza University by means of the early stage researchers funding is also gratefully acknowledged.

References

[1] Barbara Betti, Marco Pizzarelli, and Francesco Nasuti. Coupled heat transfer analysis in regeneratively cooled thrust chambers. *Journal of Propulsion and Power*, 30(2):360–367, 2014.

[2] M. P. Celano, S. Silvestri, G. Schlieben, C. Kirchberger, O. J. Haidn, and O. Knab. Injector characterization for a gaseous oxygen-methane single element combustion chamber. 8:145–164, 2016.

[3] A. Cuoci, A. Frassoldati, T. Faravelli, and E. Ranzi. Opensmoke++: An object-oriented framework for the numerical modeling of reactive systems with detailed kinetic mechanisms. *Computer Physics Communications*, 192:237–264, 2015.

[4] Zhiyu Han and Rolf D. Reitz. A temperature wall function formulation for variable-density turbulent flows with application to engine convective heat transfer modeling. *International Journal of Heat and Mass Transfer*, 40(3):613–625, 1997.

[5] G. Indelicato, P. E. Lapenna, R. Concetti, M. Caputo, M. Valorani, G. Magnotti, and F. Creta. Numerical investigation of high pressure co2-diluted combustion using a flamelet-based approach. *Combustion Science and Technology*, 2020.

[6] G. Indelicato, P.E. Lapenna, A. Remiddi, and F. Creta. An efficient modeling framework for wall heat flux prediction in rocket combustion chambers using non adiabatic flamelets and wall-functions. *International Journal of Heat and Mass Transfer*, 169:120913, 2021.

[7] G Indelicato, F Vona, A Remiddi, Lapenna P E, and F Creta. A flamelet-based numerical framework for the simulation of low-to-high mach number flows in lre. *AIAA Propulsion and Energy 2020 Forum*, 2020.

[8] Hrvoje Jasak, Aleksandar Jemcov, and Zeljko Tukovic. Openfoam: A c++ library for complex physics simulations. *International workshop on coupled methods in numerical dynamics*, pages 1–20, 11 2007.

[9] P. E. Lapenna, G. Indelicato, R. Lamioni, and F. Creta. Modeling the equations of state using a flamelet approach in lre-like conditions. *Acta Astronautica*, 158:460–469, 2019.

[10] Pasquale E Lapenna, Ruggero Amaduzzi, Diego Durigon, Giuseppe Indelicato, Francesco Nasuti, and Francesco Creta. Simulation of a single-element gch4/gox rocket combustor using a non-adiabatic flamelet method. *Joint Propulsion Conference*, page 4872, 2018.

[11] Pasquale Eduardo Lapenna and Francesco Creta. Mixing under transcritical conditions: An a-priori study using direct numerical simulation. *The Journal of Supercritical Fluids*, 128:263–278, 2017.

[12] D Lee, S Thakur, J Wright, Matthias Ihme, and Wei Shyy. Characterization of flow field structure and species composition in a shear coaxial rocket gh2/go2 injector: modeling of wall heat losses. page 6125, 2011.

[13] D. Maestro, Cuenot Benedicte, and Laurent Selle. Large eddy simulation of combustion and heat transfer in a single element gch4/gox rocket combustor. *Flow, Turbulence and Combustion*, 103, 09 2019.

[14] B. Marracino and D. Lentini. Radiation modelling in non-luminous nonpremixed turbulent flames. *Combustion Science and Technology*, 128(1-6):23–48, 1997.

[15] J. C. Oefelein and V. Yang. Modeling high-pressure mixing and combustion processes in liquid rocket engines. *Journal of Propulsion and Power*, 14(5):843–857, 1998.

DOI: 10.13009/EUCASS2022-4755

[16] Nikolaos Perakis and Oskar J. Haidn. Inverse heat transfer method applied to capacitively cooled rocket thrust chambers. *International Journal of Heat and Mass Transfer*, 131:150–166, 2019.

[17] N. Peters. Laminar diffusion flamelet models in non-premixed turbulent combustion. *Progress in Energy and Combustion Science*, 10(3):319–339, 1984.

[18] Marco Pizzarelli, Francesco Nasuti, Raffaele Votta, and Francesco Battista. Validation of conjugate heat transfer model for rocket cooling with supercritical methane. *Journal of Propulsion and Power*, 32(3):726–733, 2016.

[19] Daniel Rahn, Hendrik Riedmann, and Oskar Haidn. Conjugate heat transfer simulation of a subscale rocket thrust chamber using a timescale based frozen non-adiabatic flamelet combustion model. *AIAA Propulsion and Energy Forum*, 2019.

[20] MatjaÅ¾ RamÅ¡ak. Conjugate heat transfer of backward-facing step flow: A benchmark problem revisited. *International Journal of Heat and Mass Transfer*, 84:791–799, 2015.

[21] Arianna Remiddi, Giuseppe Indelicato, Pasquale E. Lapenna, and Francesco Creta. Effects of injector lateral confinement on lre wall heat flux characterization: numerical investigation towards data-driven modeling. *AIAA Scitech Forum*, 2021.

[22] Arianna Remiddi, Giuseppe Indelicato, Pasquale E. Lapenna, and Francesco Creta. Thermal characterization in lre: a parametric analysis on injector arrangement. *AIAA Propulsion and Energy Forum*, 2021.

[23] J. Song and B. Sun. Coupled numerical simulation of combustion and regenerative cooling in lox/methane rocket engines. *Applied Thermal Engineering*, 106:762–773, 2016.

[24] Fernanda F. Winter, Nikolaos Perakis, and Oskar J. Haidn. Emission imaging and CFD simulation of a coaxial single-element GOX/GCH4 rocket combustor. In *AIAA-paper*, page 4764, 2018.

[25] Julian Zips, Christoph Traxinger, and Michael Pfitzner. Time-resolved flow field and thermal loads in a single-element gox/gch4 rocket combustor. *International Journal of Heat and Mass Transfer*, 143, 08 2019.